Attitude control of Earth-pointing spacecraft using nonlinear H control

Mark R. Binette, Christopher J. Damaren and Lacramioara Pavel

Proceedings of the Institution of Mechanical Engineers, Part G: Journal of Aerospace Engineering published online 29 November 2013
DOI: 10.1177/0954410013513753

Original Article

Institution of MECHANICAL ENGINEERS
Journal of AEROSPACE ENGINEERING

Proc IMechE Part G:
J Aerospace Engineering
0(0) 1–15

DOI: 10.1177/0954410013513753
uk.sagepub.com/jaero
SAGE

Attitude control of Earth-pointing spacecraft using nonlinear $\mathcal{H}_\infty$ control

Mark R Binette[1], Christopher J Damaren[2] and Lacramioara Pavel[3]

Abstract

The attitude control of an Earth-pointing spacecraft in a circular orbit, subject to the gravity-gradient torque, is explored. The spacecraft attitude is described using the modified Rodrigues parameters. A series of controllers are designed using the nonlinear $\mathcal{H}_\infty$ control methodology and are subsequently generated using a Taylor series expansion to approximate solutions of the Hamilton–Jacobi equations. These controllers are applied to the problem of Earth-pointing spacecraft in circular orbits. The controllers are compared using both input–output and initial condition simulations, in an effort to gauge the improvements made possible by nonlinear feedback.

Keywords

Spacecraft attitude control, Hamilton–Jacobi equations, gravity-gradient torque, output feedback

Date received: 31 July 2013; accepted: 30 October 2013

Introduction

The dynamics that govern the rotational motion of a rigid body are well known. In particular, the evolution of the angular velocity is governed by Euler's equation, which contains a quadratic nonlinearity in that variable. There are many parameterizations for the attitude but a particularly useful approach uses the modified Rodrigues parameters (MRPs) and their corresponding shadow set.[1] This uses the minimum number of parameters (at each instant), namely three, and avoids singularity problems. The kinematical equations governing the evolution of the MRPs are identical to those for the shadow set and are polynomial in the state containing terms up to order three.

Tsiotras[2] has presented linear state feedback laws using the angular velocity and MRPs that yield asymptotic stability for inertial-pointing spacecraft. Given the nonlinear nature of Euler's equation and the MRP kinematical equations, it is tempting to speculate on the potential improvements that can be provided by nonlinear feedback laws. In this paper, the attitude control problem for Earth-pointing spacecraft is considered. The gravity-gradient torque is treated as part of the dynamics and the magnetic torque is added as a disturbance.

Over the past 20 years, much work has been applied to investigating the extension of certain linear control optimization techniques to nonlinear problems, without neglecting higher-order dynamics. One such linear control optimization technique is $\mathcal{H}_\infty$ control. $\mathcal{H}_\infty$ optimal control theory was originally formulated by Zames,[3] using an input–output framework. The solution was derived in the state space setting by Doyle et al.[4] That paper generated output feedback solutions to the suboptimal problem using two algebraic Riccati equations (AREs). As this formulation implies, the results were limited to systems for which the dynamics are linear in the state. Shortly thereafter, the state feedback results from this paper were generalized[5] to the case of general nonlinear plants, by exploiting the equivalence between the state space $\mathcal{H}_\infty$ norm and the input–output L_2-induced norm. In that work, van der Schaft replaced the relevant ARE[4] by an equivalent (nonlinear) Hamilton–Jacobi inequality. Several authors have developed methods for extending all of this work to the output feedback case. In a paper by Pavel and Fairman,[6] this is achieved by switching from the standard scattering representation of the system to the chain representation. The approach

[1]University of Toronto Institute for Aerospace Studies (UTIAS), Toronto, Ontario, Canada
[2]University of Toronto Institute for Aerospace Studies (UTIAS), Toronto, Ontario, Canada
[3]Department of Electrical and Computer Engineering, University of Toronto, Toronto, Ontario, Canada

Corresponding author:
Christopher J Damaren, University of Toronto, 4925 Dufferin Street, Toronto, ON M3H 5T6, Canada.
Email: damaren@utias.utoronto.ca

from that paper results in the need to solve a second Hamilton–Jacobi inequality.[4]

In parallel to this work on $\mathcal{H}_\infty$ control theory, many authors have attempted to incorporate nonlinear dynamics into existing control design techniques in a methodical way. One such approach is to approximate the solution of Hamilton–Jacobi equations (HJEs) through Taylor series expansions.[7–10] This approach was applied in Ref. 11 to the solution of the Hamilton–Jacobi inequality from Ref. 5. In this work, this same method will be applied to the solution of both Hamilton–Jacobi inequalities encountered in the output feedback case.

The primary purpose of this paper is to investigate a family of suboptimal nonlinear $\mathcal{H}_\infty$ controllers for Earth-pointing spacecraft attitude control, under the influence of the gravity-gradient torque. The controllers to be tested will be obtained by building on the work mentioned above.[5,6,11]

The structure of the paper is as follows: In the next section, the dynamics of an Earth-orbiting spacecraft subjected to the gravity-gradient torque are described in the orbital frame. The discussion is limited to spacecraft in circular orbits. Next, in the "Nonlinear controller determination" section, the problem to be solved in this work is defined, and the form of the controllers that will be tested will be defined. This involves applying the previously obtained results in nonlinear $\mathcal{H}_\infty$ control[5,6] to the robust attitude control problem of an Earth-pointing spacecraft. A linearized state feedback controller is derived based on a nonlinear $\mathcal{H}_\infty$ performance measure. This result is extended to higher orders of feedback by iteratively solving the higher-order terms in the relevant HJE, using a Taylor series expansion of the controller and plant dynamics[11] about the point to be controlled.

Output feedback is then considered, where a generalized nonlinear $\mathcal{H}_\infty$ control structure[6] is again linearized about the control point and extended to higher-order controllers using the same Taylor series expansions. Finally, in the "Simulation" section, the performance of these controllers is evaluated. First, the response of the controllers to initial conditions is characterized. Then, disturbance rejection properties of these controllers to unmodeled dynamics are evaluated by subjecting the system to a magnetic torque. The performance of all the controllers is then discussed, and an attempt is made to explain the underlying causes of the observed behavior.

System dynamics

This section describes the dynamics of an Earth-pointing spacecraft in a circular orbit, subject to the gravity-gradient torque.

Rigid body dynamics

To describe the dynamics of rotation of a rigid body, the body frame is defined such that the origin of the frame is at the mass centre of the spacecraft. As a matter of convenience, it is assumed that the body frame axes are aligned with the principal axes of the body. The attitude dynamics of a spacecraft subject to control torques $\mathbf{u}$ and disturbance torques $\mathbf{d}$ is given by Euler's equation:[12]

$$\dot{\boldsymbol{\omega}} = -\mathbf{I}^{-1}\boldsymbol{\omega}^{\times}\mathbf{I}\boldsymbol{\omega} + \begin{bmatrix}\mathbf{I}^{-1} & \mathbf{I}^{-1}\end{bmatrix}\begin{bmatrix}\mathbf{d}\\ \mathbf{u}\end{bmatrix} \tag{1}$$

where $\mathbf{I}$ is the constant moment of inertia matrix, $\boldsymbol{\omega}$ is the angular velocity expressed in the body-fixed frame, and

$$\boldsymbol{\omega}^{\times} = \begin{bmatrix}0 & -\omega_3 & \omega_2\\ \omega_3 & 0 & -\omega_1\\ -\omega_2 & \omega_1 & 0\end{bmatrix} \tag{2}$$

is the matrix used to implement the vector cross product. In this paper, the disturbance torques $\mathbf{d}$ are split into the modeled disturbance torques $\mathbf{d}_m$ and the unmodeled disturbance torques $\mathbf{d}_u$. The modeled disturbance torques $\mathbf{d}_m$ will be included as part of the plant for the purposes of controller design.

Modified Rodrigues parameters

The kinematics of the system will be described using the MRPs, which are derived from the earlier Cayley–Rodrigues parameters. The MRPs are attractive for several reasons. As stated in Ref. 1, they constitute a minimal, three-parameter description of the attitude of a rigid body that is non-singular for all rotations other than multiples of 2π. In addition, the MRPs are not unique: there exists a second, dynamically consistent set known as the shadow MRPs, which are singular for zero rotations, but non-singular for rotations of 2π. The dynamical consistency implies that one can switch between the MRPs and their shadow set without having to change the dynamic description of the system. By implementing such a switching procedure, it is possible to formulate non-singular optimal attitude control problems using a minimal, three-parameter description of attitude.

The MRPs σ are related to the axis $\mathbf{a}$ and rotation angle ϕ from Euler's Theorem by $\boldsymbol{\sigma} = \mathbf{a}\tan(\phi/4)$[1] The rotation matrix $\mathbf{C}$ can be described in terms of the MRPs. The relation is[13]

$$\begin{aligned}\mathbf{C} &= \mathbf{1} - 4\frac{1-\boldsymbol{\sigma}^T\boldsymbol{\sigma}}{(1+\boldsymbol{\sigma}^T\boldsymbol{\sigma})^2}\boldsymbol{\sigma}^{\times} + \frac{8}{(1+\boldsymbol{\sigma}^T\boldsymbol{\sigma})^2}\boldsymbol{\sigma}^{\times}\boldsymbol{\sigma}^{\times}\\ &= (\mathbf{1}-\boldsymbol{\sigma}^{\times})^2(\mathbf{1}+\boldsymbol{\sigma}^{\times})^{-2}\end{aligned} \tag{3}$$

where $\mathbf{1}$ is the identity matrix, and $\boldsymbol{\sigma}^{\times}$ is the skew-symmetric matrix defined according to equation (2).

The time derivative of the MRPs can be expressed using the angular velocity $\boldsymbol{\omega}$[1]:

$$\begin{aligned}\dot{\boldsymbol{\sigma}} &= \frac{1}{4}\left[(1-\boldsymbol{\sigma}^T\boldsymbol{\sigma})\mathbf{1} + 2\boldsymbol{\sigma}^{\times} + 2\boldsymbol{\sigma}\boldsymbol{\sigma}^T\right]\boldsymbol{\omega} \\ &= \mathbf{G}(\boldsymbol{\sigma})\boldsymbol{\omega}\end{aligned} \tag{4}$$

As with all three-parameter descriptions of rotation, the MRPs suffer from singularities, in this case at values of ϕ that are equal to multiples of 2π. To avoid the singularity, a different, but related description of the system, known as the shadow MRPs ($\boldsymbol{\sigma}_S$) are introduced. The shadow MRPs are related to the MRPs by

$$\boldsymbol{\sigma}_S = -\frac{\boldsymbol{\sigma}}{\boldsymbol{\sigma}^T\boldsymbol{\sigma}} \tag{5}$$

The shadow MRPs have a singularity at $\phi = 0$, so a switch from the MRPs to the shadow set is made at $\phi = \pi$. This corresponds to $\boldsymbol{\sigma}^T\boldsymbol{\sigma} = \boldsymbol{\sigma}_S^T\boldsymbol{\sigma}_S = 1$. It is not necessary to intercept the switching boundary $\boldsymbol{\sigma}^T\boldsymbol{\sigma} = 1$ exactly; it is sufficient to confirm, after each integration step, that the MRP vector does not extend outside of the unit sphere.

One very useful characteristic of the shadow MRPs is that they are dynamically consistent with the MRPs; that is they are also solutions to the differential equation in equation (4). One does not need to redefine the system dynamics to switch from using one parameterization to the other.

Orbital frame tracking

If it is desired to track a fixed direction in the orbital frame, it is convenient to express the angular velocity and attitude parameterization of the body motion relative to the orbital frame $\mathcal{F}_o$. By convention, for Earth-orbiting spacecraft the principal axes of $\mathcal{F}_o$ are defined as follows: $\hat{\mathbf{o}}_3$ points toward the Earth in the nadir direction; $\hat{\mathbf{o}}_2$ is in the opposite direction of the orbit normal; and $\hat{\mathbf{o}}_1 = \hat{\mathbf{o}}_2 \times \hat{\mathbf{o}}_3$ completes the triad. Only circular orbits[1] (i.e. with eccentricity $e = 0$) are considered in this work, where $\hat{\mathbf{o}}_1$ points in the direction of motion.

For circular orbits, the angular velocity of the spacecraft can be broken down into two components: the angular velocity relative to the orbital frame $\boldsymbol{\omega}_e$ and the angular velocity of the orbital frame itself, $-\omega_0\mathbf{o}_2$, where the orbital rate is $\omega_0 = \sqrt{\mu/R_o^3}$. Here, μ is the gravitational parameter of the primary and R_o is the orbit radius. The evolution of the angular parameterization now depends on $\boldsymbol{\omega}_e$.

The rotation matrix from the orbital frame to body frame is

$$\mathbf{C}_{bo} = [\mathbf{c}_1\ \mathbf{c}_2\ \mathbf{c}_3] \tag{6}$$

which satisfies

$$\dot{\mathbf{C}}_{bo} = -\boldsymbol{\omega}_e^{\times}\mathbf{C}_{bo} \tag{7}$$

Parameterizing $\mathbf{C}_{bo}$ by the MRPs $\boldsymbol{\sigma}$ (as in equation (3)), the kinematics become

$$\dot{\boldsymbol{\sigma}} = \frac{1}{4}[(1-\boldsymbol{\sigma}^T\boldsymbol{\sigma})\mathbf{1} + 2\boldsymbol{\sigma}^{\times} + 2\boldsymbol{\sigma}\boldsymbol{\sigma}^T]\boldsymbol{\omega}_e \tag{8}$$

Using these relations, and recalling the convention for defining the axes in the orbital frame, it is clear that the absolute angular velocity can be expressed by

$$\boldsymbol{\omega} = \boldsymbol{\omega}_e - \omega_0\mathbf{c}_2$$

Substituting $\boldsymbol{\omega}_e - \omega_0\mathbf{c}_2$ for ω in equation (1), while noting that

$$\dot{\mathbf{c}}_2 = -\boldsymbol{\omega}_e^{\times}\mathbf{c}_2 \tag{9}$$

yields

$$\begin{aligned}\dot{\boldsymbol{\omega}}_e = &-\omega_0\boldsymbol{\omega}_e^{\times}\mathbf{c}_2 - \mathbf{I}^{-1}\boldsymbol{\omega}_e^{\times}\mathbf{I}\boldsymbol{\omega}_e + \omega_0\mathbf{I}^{-1}\boldsymbol{\omega}_e^{\times}\mathbf{I}\mathbf{c}_2 \\ &+ \omega_0\mathbf{I}^{-1}\mathbf{c}_2^{\times}\mathbf{I}\boldsymbol{\omega}_e - \omega_0^2\mathbf{I}^{-1}\mathbf{c}_2^{\times}\mathbf{I}\mathbf{c}_2 \\ &+ \begin{bmatrix}\mathbf{I}^{-1} & \mathbf{I}^{-1}\end{bmatrix}\begin{bmatrix}\mathbf{d} \\ \mathbf{u}\end{bmatrix}\end{aligned} \tag{10}$$

If $\mathbf{c}_2$ is expressed in terms of the MRPs using equation (3), the dynamics relative to the orbital frame can be described using equation (10) in conjunction with the kinematics in equation (8).

Disturbance models

All spacecraft are subject to a variety of disturbance torques. The main disturbances of interest often include the gravity-gradient torque, solar-radiation pressure, magnetic torque, and aerodynamic drag. The relative effect of these disturbances varies with the distance from the primary. Hughes[12] demonstrates the relative effects of various disturbances on the attitude motion of a spacecraft for a range of Earth orbit altitudes. For this study, the focus is on the gravity-gradient and magnetic torques which are of primary importance for a wide range of geocentric orbits between *Low Earth orbit* (LEO) and *Geostationary Earth orbit* (GEO).

Gravity-gradient torque. The gravity-gradient torque occurs because the gravitational attraction of the primary affects the nearer parts of a spacecraft more strongly than it affects the further parts, in accordance with the inverse-square law. In effect, the net torque depends on the orientation of the spacecraft relative to the orbital frame. The net torque $\mathbf{G}_c$ acting on a

spacecraft can be modeled by[12]

$$\mathbf{G}_c = \frac{3\mu}{R_o^5}\mathbf{R}_0^{\times}\mathbf{I}\mathbf{R}_0 \tag{11}$$

where μ is the gravitational constant of the primary and $\mathbf{R}_0$ are the components of the spacecraft position vector in a body-fixed frame.

The gravity-gradient torque can also be expressed using the components of $\mathbf{C}_{bo}$. When expressed in the body frame $\mathbf{R}_0 = R_0\mathbf{c}_3$, with $\mathbf{c}_3$ from equation (6). Recalling that $\omega_0 = \sqrt{\mu/R_o^3}$, when the orbit is circular, gives

$$\mathbf{G}_c = \mathbf{d}_m = 3\omega_0^2\mathbf{c}_3^{\times}\mathbf{I}\mathbf{c}_3 \tag{12}$$

Note that the gravity-gradient torque $\mathbf{G}_c$ is the sole component of the modeled disturbance torque $\mathbf{d}_m$ in this paper.

Magnetic torque. The other disturbance torque that will be considered is the magnetic torque, which arises from the interaction of the Earth's magnetic field with the dipole moment of the spacecraft. The latter is caused by electromagnetism, via, for example, the current loops generated by on-board electronics. The magnitude of the dipole created is denoted by $\mathbf{m}$.

To quantify the torque generated due to the interaction of the dipole moment of the spacecraft with the Earth's magnetic field, a model is needed for the latter. To simplify the analysis, it is assumed that the Earth's magnetic field is represented as a perfect dipole located at the centre of the Earth and this dipole is aligned with true north. These assumptions lead us to a model for the magnetic field known as the untilted dipole model. It is noted in Ref. 14 that in this model, the magnetic flux density of the Earth can be expressed in the geocentric inertial frame as

$$\mathbf{B}_i = \frac{B_0}{R_0^5}\begin{bmatrix} 3xz \\ 3yz \\ 2z^2 - x^2 - y^2 \end{bmatrix} \tag{13}$$

where $B_0 \doteq -8 \times 10^{15}$ Wb·m is the strength of the field and x, y, and z are the components of the spacecraft position expressed in the geocentric inertial frame. These values can be combined to give the magnetic torque

$$\mathbf{G}_m = \mathbf{d}_u = \mathbf{m}^{\times}\mathbf{C}_{bi}\mathbf{B}_i \tag{14}$$

where care has been taken to express all quantities in the body-fixed frame. The rotation matrix $\mathbf{C}_{bi}$ can be written as $\mathbf{C}_{bo}\mathbf{C}_{oi}$ where the latter rotation matrix along with $\{x, y, z\}$ will be determined using Keplerian orbital dynamics.

Orbital frame tracking system dynamics

Combining the results from above, the attitude dynamics of a spacecraft in a circular orbit, subject to the gravity-gradient torque is

$$\begin{aligned}\dot{\boldsymbol{\omega}}_e &= -\omega_0\boldsymbol{\omega}_e^{\times}\mathbf{c}_2 - \mathbf{I}^{-1}\boldsymbol{\omega}_e^{\times}\mathbf{I}\boldsymbol{\omega}_e \\ &\quad + \omega_0\mathbf{I}^{-1}\boldsymbol{\omega}_e^{\times}\mathbf{I}\mathbf{c}_2 + \omega_0\mathbf{I}^{-1}\mathbf{c}_2^{\times}\mathbf{I}\boldsymbol{\omega}_e - \omega_0^2\mathbf{I}^{-1}\mathbf{c}_2^{\times}\mathbf{I}\mathbf{c}_2 \\ &\quad + \begin{bmatrix}\mathbf{I}^{-1} & \mathbf{I}^{-1}\end{bmatrix}\begin{bmatrix}\mathbf{d}_m + \mathbf{d}_u \\ \mathbf{u}\end{bmatrix} \\ &= -\omega_0\boldsymbol{\omega}_e^{\times}\mathbf{c}_2 - \mathbf{I}^{-1}\boldsymbol{\omega}_e^{\times}\mathbf{I}\boldsymbol{\omega}_e + \omega_0\mathbf{I}^{-1}\boldsymbol{\omega}_e^{\times}\mathbf{I}\mathbf{c}_2 \\ &\quad + \omega_0\mathbf{I}^{-1}\mathbf{c}_2^{\times}\mathbf{I}\boldsymbol{\omega}_e - \omega_0^2\mathbf{I}^{-1}\mathbf{c}_2^{\times}\mathbf{I}\mathbf{c}_2 \\ &\quad + 3\omega_0^2\mathbf{I}^{-1}\mathbf{c}_3^{\times}\mathbf{I}\mathbf{c}_3 + \begin{bmatrix}\mathbf{I}^{-1} & \mathbf{I}^{-1}\end{bmatrix}\begin{bmatrix}\mathbf{d}_u \\ \mathbf{u}\end{bmatrix}\end{aligned} \tag{15}$$

The combination of equations (8) and (15) constitutes a complete dynamic model of the system.

Nonlinear controller determination

This section describes the methodology used to develop the nonlinear controllers to be used in this paper. The starting point is a description of the general procedure for the generation of nonlinear controllers meeting the $\mathcal{H}_\infty$ control criterion. Next, this procedure is applied to the problem of orbital frame tracking subject to the gravity-gradient torque. The terminology in this section is consistent with that in the paper by LeBel and Damaren.[11]

Suboptimal $\mathcal{H}_\infty$ control problem

The analysis begins with the suboptimal $\mathcal{H}_\infty$ control problem by defining the parameters of the system. Consider a smooth nonlinear system P of the form

$$P: \begin{cases} \dot{\mathbf{x}} = \mathbf{a}(\mathbf{x}) + \mathbf{g}(\mathbf{x})\begin{bmatrix}\mathbf{w} \\ \mathbf{u}\end{bmatrix} \\ \begin{bmatrix}\mathbf{z} \\ \mathbf{y}\end{bmatrix} = \mathbf{h}(\mathbf{x}) + \mathbf{k}(\mathbf{x})\begin{bmatrix}\mathbf{w} \\ \mathbf{u}\end{bmatrix} \end{cases} \tag{16}$$

where $\mathbf{x} \in \mathbb{R}^6$ represents the state of the system, $\mathbf{u} \in \mathbb{R}^3$ are the controlled inputs to the system, $\mathbf{w} = [\mathbf{w}_1^T\ \mathbf{w}_2^T]^T \in \mathbb{R}^6$ are the exogenous inputs (including the unmodeled disturbances $\mathbf{w}_1 = \mathbf{d}_u$ and the sensor noise $\mathbf{w}_2$), $\mathbf{y} \in \mathbb{R}^3$ are the measured outputs (which will be identified with the MRPs in the sequel), $\mathbf{z} \in \mathbb{R}^9$ are the regulated outputs, and

$$\mathbf{g}(\mathbf{x}) = \begin{bmatrix}\mathbf{g}_1(\mathbf{x}) & \mathbf{g}_2(\mathbf{x})\end{bmatrix}, \quad \mathbf{h}(\mathbf{x}) = \begin{bmatrix}\mathbf{h}_1(\mathbf{x}) \\ \mathbf{h}_2(\mathbf{x})\end{bmatrix}$$

$$\mathbf{k}(\mathbf{x}) = \begin{bmatrix}\mathbf{k}_{11}(\mathbf{x}) & \mathbf{k}_{12}(\mathbf{x}) \\ \mathbf{k}_{21}(\mathbf{x}) & \mathbf{0}\end{bmatrix}$$

For the current problem, $\mathbf{k}_{11}$ and $\mathbf{k}_{12}$ are defined such that the regulated output $\mathbf{z}$ is

$$\mathbf{z} = \bar{\mathbf{h}}(\mathbf{x}, \mathbf{u}) = \begin{bmatrix} \mathbf{h}_1(\mathbf{x}) \\ \mathbf{u} \end{bmatrix} \tag{17}$$

It is assumed that there exists an equilibrium $\mathbf{x}_0$ such that $\mathbf{a}(\mathbf{x}_0) = \mathbf{0}$ and $\mathbf{h}(\mathbf{x}_0) = \mathbf{0}$. The system is represented by the block diagram in Figure 1.

Formally, the optimization problem is this: it is desired to select a control input $\mathbf{u} = \mathcal{K}(\mathbf{y})$, such that the suboptimal $\mathcal{H}_\infty$-control problem is solved. In the standard (linear) $\mathcal{H}_\infty$ control problem formulation, this amounts to ensuring that the $\mathcal{H}_\infty$ norm of the transfer function (or L_2-gain) from $\mathbf{w}$ to $\mathbf{z}$ is less than some predetermined constant $\gamma > 1$. Extending this idea to nonlinear systems simply implies that the nonlinear $\mathcal{H}_\infty$ norm (or L_2-gain) be less than γ. The $\mathcal{H}_\infty$ performance condition is summarized by the following relation

$$\int_0^T \mathbf{z}^T(t)\mathbf{z}(t)\,\mathrm{d}t \leqslant \gamma^2 \int_0^T \mathbf{w}^T(t)\mathbf{w}(t)\,\mathrm{d}t, \quad \forall \mathbf{w}(t) \in L_{2e} \tag{18}$$

There is no known closed-form solution to the optimal $\mathcal{H}_\infty$-gain optimization problem, where γ is minimal. However, given a certain value for γ, one can easily determine whether an approximate solution to the HJE exists. If the solution exists, the controller $\mathbf{u} = \mathcal{K}(\mathbf{y})$ is defined such that the L_2-gain of the system is less than the given γ. If not, an attempt is made to solve an appropriate HJE for a higher value of γ. Through an iterative process, the solution can be made to approach the optimal solution to within a desired tolerance.[11] In practice, one can select any γ greater than or equal to one, as any input affine system having L_2-gain greater than one can be made to have $\gamma = 1$ by input scaling.[6]

State feedback. Begin by initially considering the state feedback case. The measured output is taken to be $\mathbf{y} = \mathbf{x}$, leading to a controller of the form $\mathbf{u} = \mathcal{K}(\mathbf{x})$. The Hamilton–Jacobi inequality is defined as

$$\begin{aligned} H_\gamma^R(\mathbf{x}, \partial V/\partial \mathbf{x}) &\triangleq \frac{\partial V}{\partial \mathbf{x}}\mathbf{a}(\mathbf{x}) \\ &+ \frac{1}{2}\frac{\partial V}{\partial \mathbf{x}}\left[\frac{1}{\gamma^2}\mathbf{g}_1(\mathbf{x})\mathbf{g}_1^T(\mathbf{x}) - \mathbf{g}_2(\mathbf{x})\mathbf{g}_2^T(\mathbf{x})\right]\left(\frac{\partial V}{\partial \mathbf{x}}\right)^T \\ &+ \frac{1}{2}\mathbf{h}_1^T(\mathbf{x})\mathbf{h}_1(\mathbf{x}) \leqslant 0 \end{aligned} \tag{19}$$

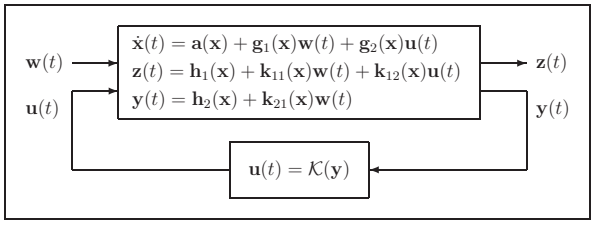

Figure 1. Block diagram of general controller with exogenous inputs.

with $\gamma > 1$. It is proved by van der Schaft[5] that, if there exists a smooth solution $V(\mathbf{x}) \geqslant 0$ satisfying the inequality in equation (19), with $V(\mathbf{x}_0) = 0$, then the state feedback

$$\mathbf{u} = -\mathbf{g}_2^T(\mathbf{x})\left(\frac{\partial V}{\partial \mathbf{x}}\right)^T \tag{20}$$

solves the suboptimal $\mathcal{H}_\infty$ control problem for the closed-loop system in equations (16), (17) and (20).

Output feedback. Extending this machinery to the output feedback case involves a change of paradigm from the common scattering representation of a system to the chain representation, via a process called the chain-scattering approach.[6] The general form of the plant remains as in equation (16).

The solution to the output feedback problem requires the solutions to two Hamilton–Jacobi inequalities. The first is identical in form to equation (19) (where we now require $V(\mathbf{x}) > 0$, $\mathbf{x} \neq \mathbf{x}_0$), and the second is

$$\begin{aligned} H_\gamma^L(\mathbf{x}, \partial U/\partial \mathbf{x}) &\triangleq \frac{\partial U}{\partial \mathbf{x}}\left(\mathbf{a}(\mathbf{x}) - \frac{1}{\gamma}\mathbf{g}_1(\mathbf{x})\mathbf{k}_2^T(\mathbf{x})\widetilde{\mathbf{R}}^{-1}(\mathbf{x})\left[\mathbf{h}_1^T\ \gamma\mathbf{h}_2^T\right]^T\right) \\ &+ \frac{1}{4}\frac{1}{\gamma^2}\frac{\partial U}{\partial \mathbf{x}}\mathbf{g}_1(\mathbf{x})\left(\mathbf{1} - \mathbf{k}_2^T(\mathbf{x})\widetilde{\mathbf{R}}^{-1}(\mathbf{x})\mathbf{k}_2(\mathbf{x})\right)\mathbf{g}_1^T(\mathbf{x})\left(\frac{\partial U}{\partial \mathbf{x}}\right)^T \\ &- \left[\mathbf{h}_1^T\ \gamma\mathbf{h}_2^T\right]\widetilde{\mathbf{R}}^{-1}(\mathbf{x})\left[\mathbf{h}_1^T\ \gamma\mathbf{h}_2^T\right]^T \leqslant 0 \end{aligned} \tag{21}$$

with $\gamma > 1$, $U(\mathbf{x}) > 0$ $(\mathbf{x} \neq \mathbf{x}_0)$, $U(\mathbf{x}_0) = 0$, and $U(\mathbf{x}) - V(\mathbf{x}) > 0$ $(\mathbf{x} \neq \mathbf{x}_0)$ and where

$$\widetilde{\mathbf{R}}(\mathbf{x}) = \begin{bmatrix} \mathbf{k}_{11}(\mathbf{x})\mathbf{k}_{11}^T(\mathbf{x}) - \mathbf{1} & \mathbf{k}_{11}(\mathbf{x})\mathbf{k}_{12}^T(\mathbf{x}) \\ \mathbf{k}_{21}(\mathbf{x})\mathbf{k}_{11}^T(\mathbf{x}) & \mathbf{k}_{21}(\mathbf{x})\mathbf{k}_{21}^T(\mathbf{x}) \end{bmatrix} \tag{22}$$

$$\mathbf{k}_2(\mathbf{x}) = \begin{bmatrix} \mathbf{k}_{11}(\mathbf{x}) \\ \mathbf{k}_{21}(\mathbf{x}) \end{bmatrix} \tag{23}$$

One possible solution to the output feedback problem is[6,15]

$$\begin{aligned} \dot{\tilde{\mathbf{x}}} &= \mathbf{a}(\tilde{\mathbf{x}}) + \left(\frac{1}{\gamma^2}\mathbf{g}_1(\tilde{\mathbf{x}})\mathbf{g}_1^T(\tilde{\mathbf{x}}) - \mathbf{g}_2(\tilde{\mathbf{x}})\mathbf{g}_2^T(\tilde{\mathbf{x}})\right)\left(\frac{\partial V}{\partial \tilde{\mathbf{x}}}\right)^T \\ &\quad + \mathbf{L}_0(\tilde{\mathbf{x}})[\gamma\mathbf{h}_2(\tilde{\mathbf{x}}) - \gamma\mathbf{y}] \\ \mathbf{u} &= -\mathbf{g}_2^T(\tilde{\mathbf{x}})\left(\frac{\partial V}{\partial \tilde{\mathbf{x}}}\right)^T \end{aligned} \tag{24}$$

where $\mathbf{L}_0(\mathbf{x})$ is chosen to satisfy

$$\left[\frac{\partial U}{\partial \mathbf{x}} - \frac{\partial V}{\partial \mathbf{x}}\right]\mathbf{L}_0(\mathbf{x}) = -\gamma\mathbf{h}_2^T(\mathbf{x}) \tag{25}$$

The system defined by equations (16) and (24) solves the suboptimal nonlinear $\mathcal{H}_\infty$ control problem.

From this treatment, it is clear that the selection of the form of $\mathbf{g}_2(\mathbf{x})$ and $\mathbf{h}(\mathbf{x})$ amounts to the selection of weighting criteria for the control effort and outputs, respectively, and thus must be carefully made.

Control of rigid body attitude

In the attitude control problem being considered in this work, $\mathbf{x} = \begin{bmatrix}\boldsymbol{\omega}_e^T & \boldsymbol{\sigma}^T\end{bmatrix}^T$ and $\mathbf{w} = \begin{bmatrix}\mathbf{w}_1^T & \mathbf{w}_2^T\end{bmatrix}^T$ where $\mathbf{w}_1 = \mathbf{d}_u$ and $\mathbf{w}_2$ is the sensor noise to be introduced below. Using equations (8) and (15), gives

$$\begin{aligned}\mathbf{a}(\mathbf{x}) &= \begin{bmatrix} -\omega_0\boldsymbol{\omega}_e^{\times}\mathbf{c}_2 - \mathbf{I}^{-1}\boldsymbol{\omega}_e^{\times}\mathbf{I}\boldsymbol{\omega}_e + \omega_0\mathbf{I}^{-1}\boldsymbol{\omega}_e^{\times}\mathbf{I}\mathbf{c}_2 \\ +\omega_0\mathbf{I}^{-1}\mathbf{c}_2^{\times}\mathbf{I}\boldsymbol{\omega}_e - \omega_0^2\mathbf{I}^{-1}\mathbf{c}_2^{\times}\mathbf{I}\mathbf{c}_2 \\ +3\omega_0^2\mathbf{I}^{-1}\mathbf{c}_3^{\times}\mathbf{I}\mathbf{c}_3 \\ \tfrac{1}{4}[(1-\boldsymbol{\sigma}^T\boldsymbol{\sigma})\mathbf{1} + 2\boldsymbol{\sigma}^{\times} + 2\boldsymbol{\sigma}\boldsymbol{\sigma}^T]\boldsymbol{\omega}_e \end{bmatrix} \\ \mathbf{g}_1(\mathbf{x}) &= \begin{bmatrix}\mathbf{I}^{-1} & \mathbf{0} \\ \mathbf{0} & \mathbf{0}\end{bmatrix} \\ \mathbf{g}_2(\mathbf{x}) &= \begin{bmatrix}\mathbf{I}^{-1} \\ \mathbf{0}\end{bmatrix} = \mathbf{B}\end{aligned} \tag{26}$$

The quantities $\mathbf{h}_1(\mathbf{x})$ and $\mathbf{k}(\mathbf{x})$ are taken to be

$$\mathbf{h}_1(\mathbf{x}) = \mathbf{H}\mathbf{x} = \begin{bmatrix}q_1\mathbf{1} & \mathbf{0} \\ \mathbf{0} & q_2\mathbf{1}\end{bmatrix}\begin{bmatrix}\boldsymbol{\omega}_e \\ \boldsymbol{\sigma}\end{bmatrix} \tag{27}$$

$$\mathbf{k}(\mathbf{x}) = \begin{bmatrix}\mathbf{0} & \mathbf{0} & \mathbf{0} \\ \mathbf{0} & \mathbf{0} & \mathbf{1} \\ \mathbf{0} & \mathbf{1} & \mathbf{0}\end{bmatrix} \tag{28}$$

where $q_1 > 0$ and $q_2 > 0$ are appropriately selected weighting values. Thus, the equilibrium is at $\mathbf{x}_0 = \begin{bmatrix}\mathbf{0}^T & \mathbf{0}^T\end{bmatrix}^T$

The state feedback controller in equation (20) is of the form

$$\mathbf{u} = -\mathbf{B}^T\left(\frac{\partial V}{\partial \mathbf{x}}\right)^T \tag{29}$$

where $\partial V(\mathbf{x})/\partial\mathbf{x}$ is a solution to the following HJE obtained from (19)

$$2\frac{\partial V}{\partial \mathbf{x}}\mathbf{a}(\mathbf{x}) - \frac{\partial V}{\partial \mathbf{x}}\mathbf{R}_1\left(\frac{\partial V}{\partial \mathbf{x}}\right)^T + \mathbf{x}^T\mathbf{S}_1\mathbf{x} = 0 \tag{30}$$

where

$$\mathbf{R}_1 = \mathbf{B}\mathbf{B}^T - \frac{1}{\gamma^2}\mathbf{g}_1(\mathbf{x})\mathbf{g}_1(\mathbf{x})^T = \frac{\gamma^2 - 1}{\gamma^2}\mathbf{B}\mathbf{B}^T \tag{31}$$

$$\mathbf{S}_1 = \mathbf{H}^T\mathbf{H} \tag{32}$$

Note that in equation (30), the equality version of equation (19) is being solved.

For the output feedback case, the measured output $\mathbf{y}$ is defined as

$$\begin{aligned}\mathbf{y} &= \mathbf{h}_2(\mathbf{x}) + \mathbf{w}_2(t) = \mathbf{C}\mathbf{x} + \mathbf{w}_2(t) \\ &= \begin{bmatrix}\mathbf{0} & q_3\mathbf{1}\end{bmatrix}\begin{bmatrix}\boldsymbol{\omega}_e \\ \sigma\end{bmatrix} + \mathbf{w}_2(t)\end{aligned} \tag{33}$$

where $q_3 > 0$ permits scaling of the relative size of the exact measurement of the MRPs and the sensor noise $\mathbf{w}_2(t)$. Alternatively, a factor could have been included in the (3,2) partition of $\mathbf{k}(\mathbf{x})$ in equation (28). It has been ensured that the measured outputs include the attitude measurements, in order to maintain detectability. The state estimator from equation (24) has the form

$$\dot{\tilde{\mathbf{x}}} = \mathbf{a}(\tilde{\mathbf{x}}) - \mathbf{R}_1\left[\frac{\partial V}{\partial \tilde{\mathbf{x}}}(\tilde{\mathbf{x}})\right]^T + \mathbf{L}_0(\tilde{\mathbf{x}})[\gamma\mathbf{C}\tilde{\mathbf{x}} - \gamma\mathbf{y}] \tag{34}$$

As with the state feedback case, one can make substitutions into equation (21) and simplify it to

$$2\frac{\partial U}{\partial \mathbf{x}}\mathbf{a}(\mathbf{x}) - \frac{\partial U}{\partial \mathbf{x}}\mathbf{R}_2\left(\frac{\partial U}{\partial \mathbf{x}}\right)^T + \mathbf{x}^T\mathbf{S}_2\mathbf{x} = 0 \tag{35}$$

where

$$\mathbf{R}_2 = -\frac{1}{\gamma^2}\mathbf{g}_1(\mathbf{x})\mathbf{g}_1(\mathbf{x})^T = -\frac{1}{\gamma^2}\mathbf{B}\mathbf{B}^T \tag{36}$$

$$\mathbf{S}_2 = \mathbf{H}^T\mathbf{H} - \gamma^2\mathbf{C}^T\mathbf{C} \tag{37}$$

Note that the equality version of equation (21) is being solved here.

Taylor series expansions. Unfortunately, it has proved impossible to solve equations (30) and (35) analytically due to the nonlinearities present in $\mathbf{a}(\mathbf{x})$ (which will in turn lead to nonlinearities in $\partial V/\partial\mathbf{x}$ and $\partial U/\partial\mathbf{x}$). Therefore, a Taylor series expansion of all three quantities is employed, in order to obtain a useful result. It will be assumed that all three of them are smooth (infinitely differentiable).

Begin by taking a Taylor series expansion to $\mathbf{a}(\mathbf{x})$ about $\mathbf{x} = \mathbf{0}$

$$\begin{aligned}\mathbf{a}(\mathbf{x}) &\doteq \mathbf{a}_1(\mathbf{x}) + \mathbf{a}_2(\mathbf{x}) + \mathbf{a}_3(\mathbf{x}) + \mathbf{a}_4(\mathbf{x}) \\ &= \mathbf{A}_1\mathbf{x} + \mathrm{col}_k\{\mathbf{x}^T\mathbf{A}_{2k}\mathbf{x}\} + \mathrm{mat}_{ab}\{\mathbf{x}^T\mathbf{A}_{3ab}\mathbf{x}\}\mathbf{x} \\ &\quad + \mathrm{col}_k\{\mathbf{x}^T\mathrm{mat}_{ab}\{\mathbf{x}^T\mathbf{A}_{4kab}\mathbf{x}\}\mathbf{x}\}\end{aligned} \tag{38}$$

where the first four terms have been listed. The symbol col_k indicates a column vector with index k, and mat_{ab} indicates a matrix with row index a and column index b.

Consider the following definition

$$\mathbf{E} = \begin{bmatrix}E_1 \\ E_2 \\ E_3\end{bmatrix} = \begin{bmatrix}(I_2 - I_3)/I_1 \\ (I_3 - I_1)/I_2 \\ (I_1 - I_2)/I_3\end{bmatrix}$$

where I_i is the moment of inertia corresponding to the ith principal axis of the body. Using this definition, one can express the first four terms of $\mathbf{a}(\mathbf{x})$ in the orbital frame tracking problem in terms of the components of the angular rate and MRPs. Note that the term $(1+\boldsymbol{\sigma}^T\boldsymbol{\sigma})^{-2}$ from equation (3) has the following third-order Taylor expansion about $\boldsymbol{\sigma}=\mathbf{0}$

$$\left(1+\boldsymbol{\sigma}^T\boldsymbol{\sigma}\right)^{-2} \doteq 1-2\boldsymbol{\sigma}^T\boldsymbol{\sigma} \tag{39}$$

which yields the following Taylor expansions for $\mathbf{a}(\mathbf{x})$ defined in equation (26), accurate to fourth-order:

$$\mathbf{a}_1(\mathbf{x}) = \begin{bmatrix} -16E_1\omega_0^2\sigma_1 - (E_1-1)\omega_0\omega_{e3} \\ 12E_2\omega_0^2\sigma_2 \\ 4E_3\omega_0^2\sigma_3 - (E_3+1)\omega_0\omega_{e1} \\ \omega_{e1}/4 \\ \omega_{e2}/4 \\ \omega_{e3}/4 \end{bmatrix} \tag{40}$$

$$\mathbf{a}_2(\mathbf{x}) = \begin{bmatrix} E_1\omega_{e2}\omega_{e3} + 4(E_1+1)\omega_0\omega_{e2}\sigma_1 - 16E_1\omega_0^2\sigma_2\sigma_3 \\ E_2\omega_{e1}\omega_{e3} - 4(E_2+1)\omega_0\omega_{e3}\sigma_3 + 4(E_2-1)\omega_0\omega_{e1}\sigma_1 - 40E_2\omega_0^2\sigma_1\sigma_3 \\ E_3\omega_{e1}\omega_{e2} - 4(E_3-1)\omega_0\omega_{e2}\sigma_3 + 56E_3\omega_0^2\sigma_1\sigma_2 \\ -\omega_{e2}\sigma_3/2 + \omega_{e3}\sigma_2/2 \\ \omega_{e1}\sigma_3/2 - \omega_{e3}\sigma_1/2 \\ -\omega_{e1}\sigma_2/2 + \omega_{e2}\sigma_1/2 \end{bmatrix} \tag{41}$$

$$\mathbf{a}_3(\mathbf{x}) = \begin{bmatrix} E_1\omega_0^2\sigma_1(176\sigma_1^2+144\sigma_2^2+80\sigma_3^2) - 8(E_1+1)\omega_0\omega_{e2}\sigma_2\sigma_3 + 8(E_1-1)\omega_0\omega_{e3}(\sigma_1^2+\sigma_3^2) \\ E_2\omega_0^2\sigma_2(-164\sigma_1^2-132\sigma_2^2-4\sigma_3^2) - 8(E_2+1)\omega_0\omega_{e3}\sigma_1\sigma_2 - 8(E_2-1)\omega_0\omega_{e1}\sigma_2\sigma_3 \\ E_3\omega_0^2\sigma_3(-140\sigma_1^2+84\sigma_2^2-44\sigma_3^2) - 8(E_3-1)\omega_0\omega_{e2}\sigma_1\sigma_2 + 8(E_3+1)\omega_0\omega_{e1}(\sigma_1^2+\sigma_3^2) \\ \omega_{e1}(\sigma_1^2-\sigma_2^2-\sigma_3^2)/4 + \omega_{e2}\sigma_1\sigma_2/2 + \omega_{e3}\sigma_1\sigma_3/2 \\ \omega_{e2}(-\sigma_1^2+\sigma_2^2-\sigma_3^2)/4 + \omega_{e1}\sigma_1\sigma_2/2 + \omega_{e3}\sigma_2\sigma_3/2 \\ \omega_{e3}(-\sigma_1^2-\sigma_2^2+\sigma_3^2)/4 + \omega_{e1}\sigma_1\sigma_3/2 + \omega_{e2}\sigma_2\sigma_3/2 \end{bmatrix} \tag{42}$$

$$\mathbf{a}_4(\mathbf{x}) = \begin{bmatrix} E_1\omega_0^2\sigma_2\sigma_3(160\sigma_1^2+224\sigma_2^2-32\sigma_3^2) \\ -12(E_1+1)\omega_0\omega_{e2}\sigma_1(\sigma_1^2+\sigma_2^2+\sigma_3^2) \\ E_2\omega_0^2\sigma_1\sigma_3(336\sigma_1^2+400\sigma_2^2+144\sigma_3^2) \\ +12\omega_0((E_2+1)\omega_{e3}\sigma_3 - (E_2-1)\omega_{e1}\sigma_1)(\sigma_1^2+\sigma_2^2+\sigma_3^2) \\ E_3\omega_0^2\sigma_1\sigma_2(-368\sigma_1^2-304\sigma_2^2-560\sigma_3^2) \\ +12(E_3-1)\omega_0\omega_{e2}\sigma_3(\sigma_1^2+\sigma_2^2+\sigma_3^2) \\ 0 \\ 0 \\ 0 \end{bmatrix} \tag{43}$$

The Taylor series expansion of the solutions to the HJEs in equations (30) and (35) have similar forms to that of $\mathbf{a}(\mathbf{x})$. The fourth-order Taylor series expansion of $\partial V/\partial\mathbf{x}$ is[11]

$$\begin{aligned} \partial V/\partial\mathbf{x} &\doteq \nabla\mathbf{V}_1(\mathbf{x}) + \nabla\mathbf{V}_2(\mathbf{x}) + \nabla\mathbf{V}_3(\mathbf{x}) + \nabla\mathbf{V}_4(\mathbf{x}) \\ &= \mathbf{x}^T\mathbf{P}_1 + \mathrm{row}_k\left\{\mathbf{x}^T\mathbf{P}_{2k}\mathbf{x}\right\} \\ &\quad + \mathbf{x}^T\mathrm{mat}_{ab}\left\{\mathbf{x}^T\mathbf{P}_{3ab}\mathbf{x}\right\} \\ &\quad + \mathrm{row}_k\left\{\mathbf{x}^T\mathrm{mat}_{ab}\left\{\mathbf{x}^T\mathbf{P}_{4kab}\mathbf{x}\right\}\mathbf{x}\right\} \end{aligned} \tag{44}$$

Equivalently, the expansion for $\partial U/\partial\mathbf{x}$ is

$$\begin{aligned} \partial U/\partial\mathbf{x} &\doteq \nabla\mathbf{U}_1(\mathbf{x}) + \nabla\mathbf{U}_2(\mathbf{x}) + \nabla\mathbf{U}_3(\mathbf{x}) + \nabla\mathbf{U}_4(\mathbf{x}) \\ &= \mathbf{x}^T\mathbf{Q}_1 + \mathrm{row}_k\left\{\mathbf{x}^T\mathbf{Q}_{2k}\mathbf{x}\right\} + \mathbf{x}^T\mathrm{mat}_{ab}\left\{\mathbf{x}^T\mathbf{Q}_{3ab}\mathbf{x}\right\} \\ &\quad + \mathrm{row}_k\left\{\mathbf{x}^T\mathrm{mat}_{ab}\left\{\mathbf{x}^T\mathbf{Q}_{4kab}\mathbf{x}\right\}\mathbf{x}\right\} \end{aligned} \tag{45}$$

With the above expansions in hand, the observer gain defined in equation (25) is given by

$$\mathbf{L}_0(\mathbf{x}) = -\gamma\begin{bmatrix} (\mathbf{Q}_1-\mathbf{P}_1) + \mathrm{row}_k\{(\mathbf{Q}_{2k}-\mathbf{P}_{2k})\mathbf{x}\} \\ +\mathrm{mat}_{ab}\{\mathbf{x}^T(\mathbf{Q}_{3ab}-\mathbf{P}_{3ab})\mathbf{x}\} \\ +\mathrm{row}_k\{\mathrm{mat}_{ab}\{\mathbf{x}^T(\mathbf{Q}_{4kab}-\mathbf{P}_{4kab})\mathbf{x}\}\mathbf{x}\} \end{bmatrix}^{-1}\mathbf{C}^T \tag{46}$$

First-order controller. To obtain a linear controller that solves the $\mathcal{H}_\infty$ problem locally, replace $\mathbf{a}(\mathbf{x})$, $\partial V/\partial\mathbf{x}$, and $\partial U/\partial\mathbf{x}$ by their respective Taylor series expansions in equations (30) and (35) and focus attention on those terms in the expansions that are quadratic in the states. To calculate the $\nabla\mathbf{V}_1(\mathbf{x})$ term, look at the terms in the Taylor series approximation to equation (30) that are quadratic in the states. From this, one recovers the familiar ARE:

$$\mathbf{P}_1\mathbf{A}_1 + \mathbf{A}_1^T\mathbf{P}_1 - \mathbf{P}_1\mathbf{R}_1\mathbf{P}_1 + \mathbf{S}_1 = \mathbf{0} \tag{47}$$

The $\nabla \mathbf{U}_1(\mathbf{x})$ term can also be calculated by looking at the quadratic terms in equation (35)

$$\mathbf{Q}_1\mathbf{A}_1 + \mathbf{A}_1^T\mathbf{Q}_1 - \mathbf{Q}_1\mathbf{R}_2\mathbf{Q}_1 + \mathbf{S}_2 = \mathbf{0} \tag{48}$$

In practice, the filtering form of this equation is solved for $\mathbf{Q}_1^{-1}$ (which is obtained by pre- and post-multiplying equation (48) by $\mathbf{Q}_1^{-1}$).

Iterative approach for higher-order controllers. Higher-order terms in equations (44) and (45) are found iteratively using the higher-order terms in the Taylor series expansions of equations (30) and (35), respectively.

The second-order solutions are given by

$$\mathbf{P}_2^{(i,j)} = -\mathbf{A}_2^{(i,j)T}\mathbf{P}_1\mathbf{A}_{cs1}^{-1} \tag{49}$$

$$\mathbf{Q}_2^{(i,j)} = -\mathbf{A}_2^{(i,j)T}\mathbf{Q}_1\mathbf{A}_{co1}^{-1} \tag{50}$$

where

$$\mathbf{P}_2^{(i,j)} = \mathrm{row}_k\left\{P_{2k}^{(i,j)}\right\}, \quad \mathbf{Q}_2^{(i,j)} = \mathrm{row}_k\left\{Q_{2k}^{(i,j)}\right\}$$
$$\mathbf{A}_{cs1} = \mathbf{A}_1 - \mathbf{R}_1\mathbf{P}_1, \quad \mathbf{A}_{co1} = \mathbf{A}_1 - \mathbf{R}_2\mathbf{Q}_1$$
$$\mathbf{A}_2^{(i,j)} = \mathrm{col}_k\left\{A_{2k}^{(i,j)}\right\}$$

The third-order solutions are given by

$$\mathbf{P}_3^{(i,j)} = -\left[\mathrm{mat}_{ab}\left\{\mathbf{P}_2^{(a,i)}\mathbf{A}_{cs2}^{(j,b)}\right\} + \mathbf{P}_1\mathbf{A}_3^{(i,j)}\right]\mathbf{A}_{cs1}^{-1} \tag{51}$$

$$\mathbf{Q}_3^{(i,j)} = -\left[\mathrm{mat}_{ab}\left\{\mathbf{Q}_2^{(a,i)}\mathbf{A}_{co2}^{(j,b)}\right\} + \mathbf{Q}_1\mathbf{A}_3^{(i,j)}\right]\mathbf{A}_{co1}^{-1} \tag{52}$$

where

$$\mathbf{P}_3^{(i,j)} = \mathrm{mat}_{ab}\left\{P_{3ab}^{(i,j)}\right\}, \mathbf{Q}_3^{(i,j)} = \mathrm{mat}_{ab}\left\{Q_{3ab}^{(i,j)}\right\}$$
$$\mathbf{A}_{cs2}^{(j,b)} = \mathbf{A}_2^{(j,b)} - \frac{1}{2}\mathbf{R}_1\mathbf{P}_{2k}^{(j,b)T},$$
$$\mathbf{A}_{co2}^{(j,b)} = \mathbf{A}_2^{(j,b)} - \frac{1}{2}\mathbf{R}_2\mathbf{Q}_2^{(j,b)T}$$
$$\mathbf{A}_3^{(i,j)} = \mathrm{mat}_{ab}\left\{A_{3ab}^{(i,j)}\right\}$$

Finally, the fourth-order solutions are given by

$$\mathrm{mat}_{ak}\{P_{4kab}^{(i,j)}\} = -\left[\begin{array}{l}\mathrm{mat}_{ak}\left\{\mathbf{P}_{3a}^{(i,j)}\mathbf{A}_{cs2}^{(b,k)}\right\} \\ \quad +\mathrm{mat}_{ak}\left\{\mathbf{P}_2^{(a,i)}\mathbf{A}_{cs3k}^{(j,b)}\right\} + \mathrm{mat}_{ak}\{A_{4kab}^{(i,j)}\}\mathbf{P}_1\end{array}\right]\mathbf{A}_{cs1}^{-1} \tag{53}$$

$$\mathrm{mat}_{ak}\{Q_{4kab}^{(i,j)}\} = -\left[\begin{array}{l}\mathrm{mat}_{ak}\left\{\mathbf{Q}_{3a}^{(i,j)}\mathbf{A}_{co2}^{(b,k)}\right\} \\ \quad +\mathrm{mat}_{ak}\left\{\mathbf{Q}_2^{(a,i)}\mathbf{A}_{co3k}^{(j,b)}\right\} + \mathrm{mat}_{ak}\{A_{4kab}^{(i,j)}\}\mathbf{Q}_1\end{array}\right]\mathbf{A}_{co1}^{-1} \tag{54}$$

where

$$\mathbf{A}_{cs3k}^{(j,b)} = \mathbf{A}_{3k}^{(j,b)} - \frac{1}{2}\mathbf{R}_1\mathbf{P}_{3k}^{(j,b)},$$
$$\mathbf{A}_{co2k}^{(j,b)} = \mathbf{A}_{3k}^{(j,b)} - \frac{1}{2}\mathbf{R}_2\mathbf{Q}_{3k}^{(j,b)}$$
$$\mathbf{P}_{3k}^{(i,j)} = \mathrm{row}_a\left\{P_{3ka}^{(i,j)}\right\}, \quad \mathbf{Q}_{3k}^{(i,j)} = \mathrm{row}_a\left\{Q_{3ka}^{(i,j)}\right\}$$
$$\mathbf{A}_{3k}^{(i,j)} = \mathrm{col}_a\left\{A_{3ak}^{(i,j)}\right\}$$

Non-uniqueness of Taylor series expansions

Unfortunately, the Taylor series expansions for $\mathbf{a}_2(\mathbf{x})$, $\mathbf{a}_3(\mathbf{x})$, or $\mathbf{a}_4(\mathbf{x})$ are not unique. For instance, the $-\frac{1}{2}\sigma_3\omega_{e2}$ term from the fourth row of $\mathbf{a}_2(\mathbf{x})$ can be distributed to either element $\mathbf{A}_{24}^{(6,2)}$ or element $\mathbf{A}_{24}^{(2,6)}$ in the Taylor expansion.

This non-uniqueness in the expansion of $\mathbf{a}(\mathbf{x})$ leads naturally to non-uniqueness in the solution to the Hamilton–Jacobi inequalities (30) and (35). This highlights another reason for which the solution posed in this paper is suboptimal. Although the $\mathcal{H}_\infty$ control problem is still solved locally for any distribution of terms in the Taylor series expansion of $\mathbf{a}(\mathbf{x})$, the controllers do have measurably different performance when the terms are moved.

Simulation

In this section, the various orders of the controller are compared through numerical simulation. The performance measures to be used in the analysis are presented here. An analysis is then performed of the relative performance of the various controllers when subjected to a tumbling initial condition, followed by an analysis of relative performance when subjected to magnetic disturbance torques. Throughout the simulations, perfect knowledge of the inertia matrix is assumed and the body frame axes are aligned accordingly

$$\mathbf{I} = \begin{bmatrix} 10 & 0 & 0 \\ 0 & 6.3 & 0 \\ 0 & 0 & 8.5 \end{bmatrix} \mathrm{kg}\cdot\mathrm{m}^2$$

The chosen controller design parameters are $q_1 = q_2 = 0.01$ and $q_3 = 10$. For the state feedback controller, $\gamma = 2$ and for the output feedback controller, $\gamma = 20$. Sensor noise will not be included in the simulations.

Description of performance metrics

To evaluate the relative performance of these several controllers, a series of performance metrics has been developed. Primary among these are the numerically integrated L_2-norm values for

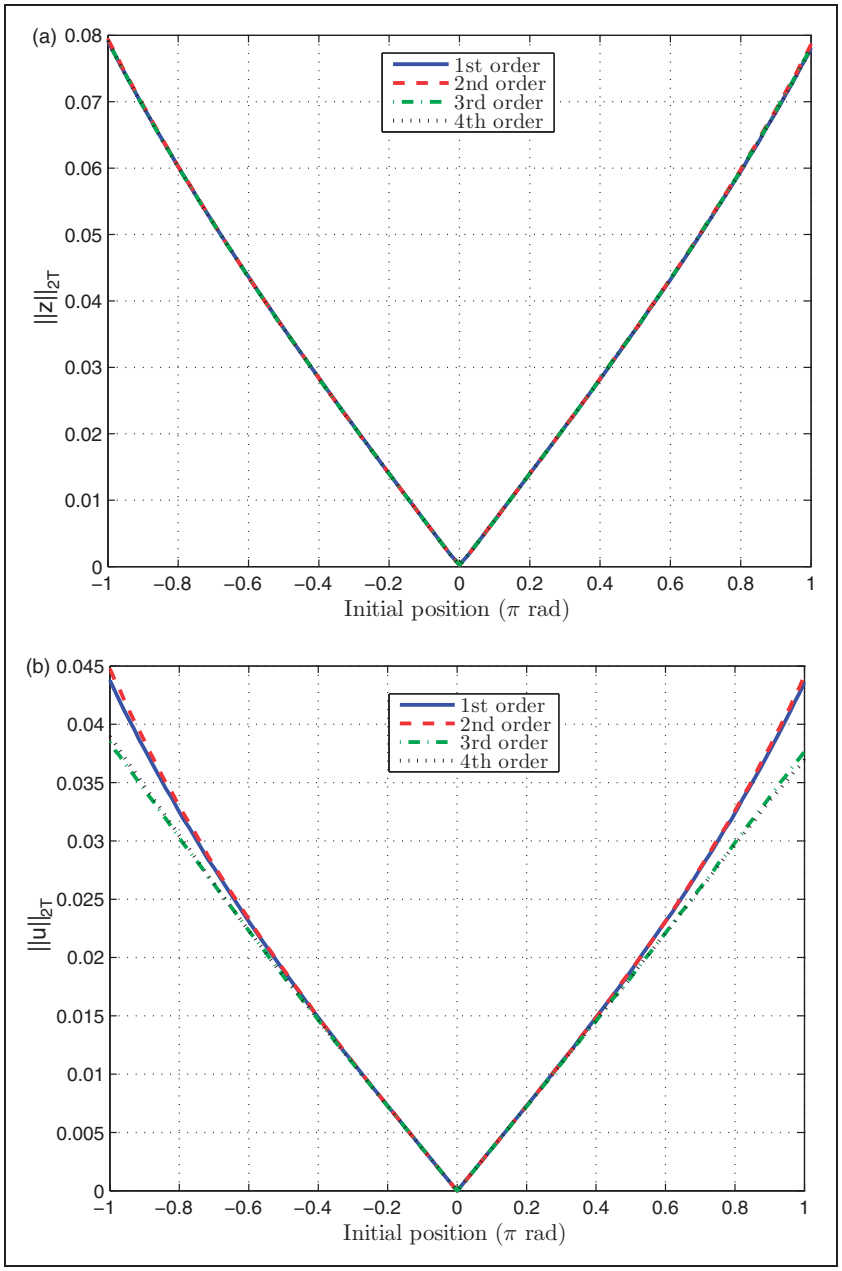

Figure 2. Relative performance for various initial values of σ for the state feedback controllers tracking an orbitally fixed direction. (a) $||\mathbf{z}||_{2T}$ response and (b) $||\mathbf{w}||_{2T}$ response.

the various parameters. The terms to be used are the following

$$||\boldsymbol{\omega}_e||_{2T} = \left[\int_0^T \boldsymbol{\omega}_e^T(t)\boldsymbol{\omega}_e(t)\mathrm{d}t\right]^{1/2}$$

$$||\phi||_{2T} = \left[\int_0^T \phi^2\, dt\right]^{1/2}$$

$$||\mathbf{u}||_{2T} = \left[\int_0^T \mathbf{u}^T(t)\mathbf{u}(t)\mathrm{d}t\right]^{1/2}$$

$$||\mathbf{w}||_{2T} = \left[\int_0^T \mathbf{w}^T(t)\mathbf{w}(t)\mathrm{d}t\right]^{1/2}, \quad \mathbf{w} = [\mathbf{d}_u^T\ \mathbf{0}^T]$$

$$||\mathbf{z}||_{2T} = \left[\int_0^T \mathbf{z}^T(t)\mathbf{z}(t)\mathrm{d}t\right]^{1/2}$$

The ϕ parameter is used instead of the MRPs, as switching from MRPs to shadow MRPs instantaneously changes the desired equilibrium. Note that ϕ is the angle of rotation in Euler's Theorem. The value selected for T will be the orbital period.

It is also of interest to verify that the nonlinear $\mathcal{H}_\infty$ gain of the system remains less than γ, by calculating the closed-loop gain as a performance metric

$$\mathrm{CL}-\mathrm{gain} = ||\mathbf{z}||_{2T}/||\mathbf{w}||_{2T} \tag{55}$$

Response to initial conditions

The controller performance as a function of the initial conditions will now be characterized. Note that this

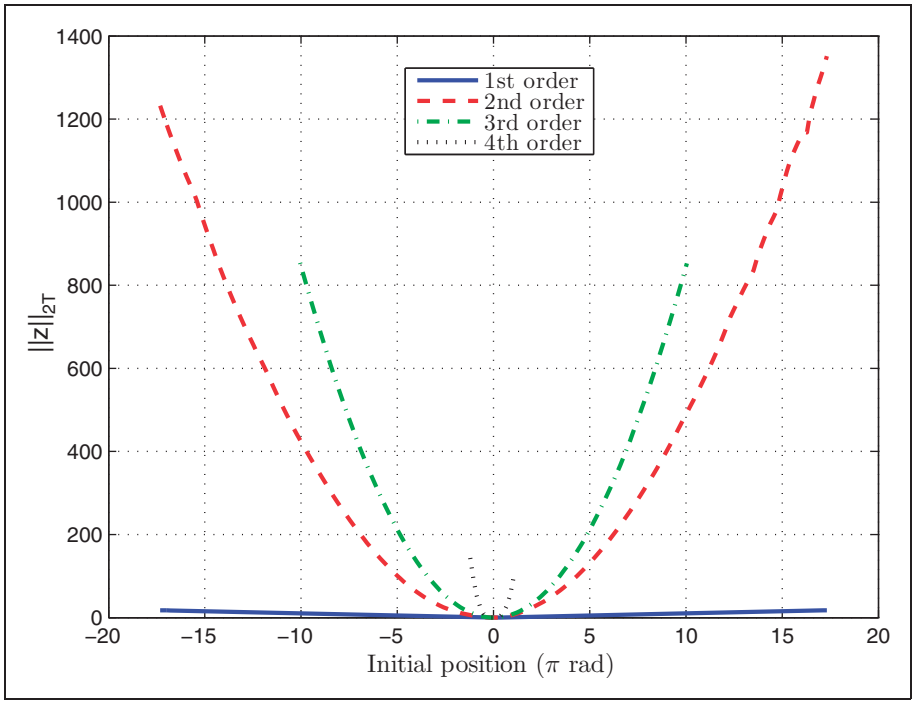

Figure 3. $||\mathbf{z}||_{2T}$ response for various initial values of ω_e for the state feedback controllers tracking an orbitally fixed direction.

was not considered in the framework used to define the controllers. However, the inclusion of the previously unmodeled nonlinear dynamics in the higher-order controllers could be expected to result in better performance far from the equilibrium, due to the local nature of the linearized result. The effects of disturbance torques will be ignored in this portion of the analysis.

State feedback. A comparison of the various controllers for various ranges of initial attitude will first be considered. The initial angular rate $\boldsymbol{\omega}_e$ is set to $\mathbf{0}$ and, using the parameters $\mathbf{a}$ and ϕ from Euler's Theorem, the initial angle is varied such that $-\pi \leqslant \phi \leqslant \pi$ about axis $\mathbf{a} = [0.4855, 0.2015, 0.8507]^T$. For $|\phi| > \pi$, the controller would switch to the shadow parameters and the response would be identical to that of $\phi \pm 2\pi$. The results for various initial conditions are presented in Figure 2.

As the figure shows, the control effort and performance measures climb steadily as ϕ approaches π. Note that the third- and fourth-order controllers do have slightly improved performance relative to the control effort required to return the system to the origin. However, as the total output norm value does not change, there is a trade-off in terms of the response speed (the higher-order controllers respond more slowly, given $\mathbf{A}$ matrix values that are evenly distributed).

Next, consider the domain of attraction of the controllers with respect to the initial angular velocity relative to the orbital frame, $\boldsymbol{\omega}_e$. In this case, there is a significant variation in performance when the nonlinear dynamics of the system are included. Unfortunately, the simulation results do not support the assumption that increasing the order of the controller necessarily improves the performance so achieved. The results are summarized in Figure 3. The three higher-order controllers show significantly reduced performance from a regulated variable perspective, when compared to the first-order controller. The simulation eventually breaks down for the higher-order controllers.

Output feedback. Figure 4 demonstrates the response of the output feedback controller to variations in the initial attitude, using the same simulation parameters as in the previous section.

The output feedback response is quite different from the state feedback response. The first-order output feedback controller works as effectively as the state feedback controllers. However, for the nonlinear controllers, there is much more risk that the $(\mathbf{Q}(\tilde{\mathbf{x}}) - \mathbf{P}(\tilde{\mathbf{x}}))^{-1}$ term in the observer (see equation (46)) is (nearly) degenerate, as the matrices are no longer constant. As a result, the domain of attraction is reduced significantly, and Figure 4 is reduced in scale accordingly. The changes in regions of stability for the various controllers do not seem to depend on only the order of the controller. For instance, in this simulation, the second-order output feedback controller has the smallest region of stability.

When one looks at the output feedback response to varying the initial angular velocity, the results are quite different from the state feedback response. From Figure 5, it is noted that the region of stability for the controller is quite small compared to some of the initial conditions that may be encountered in

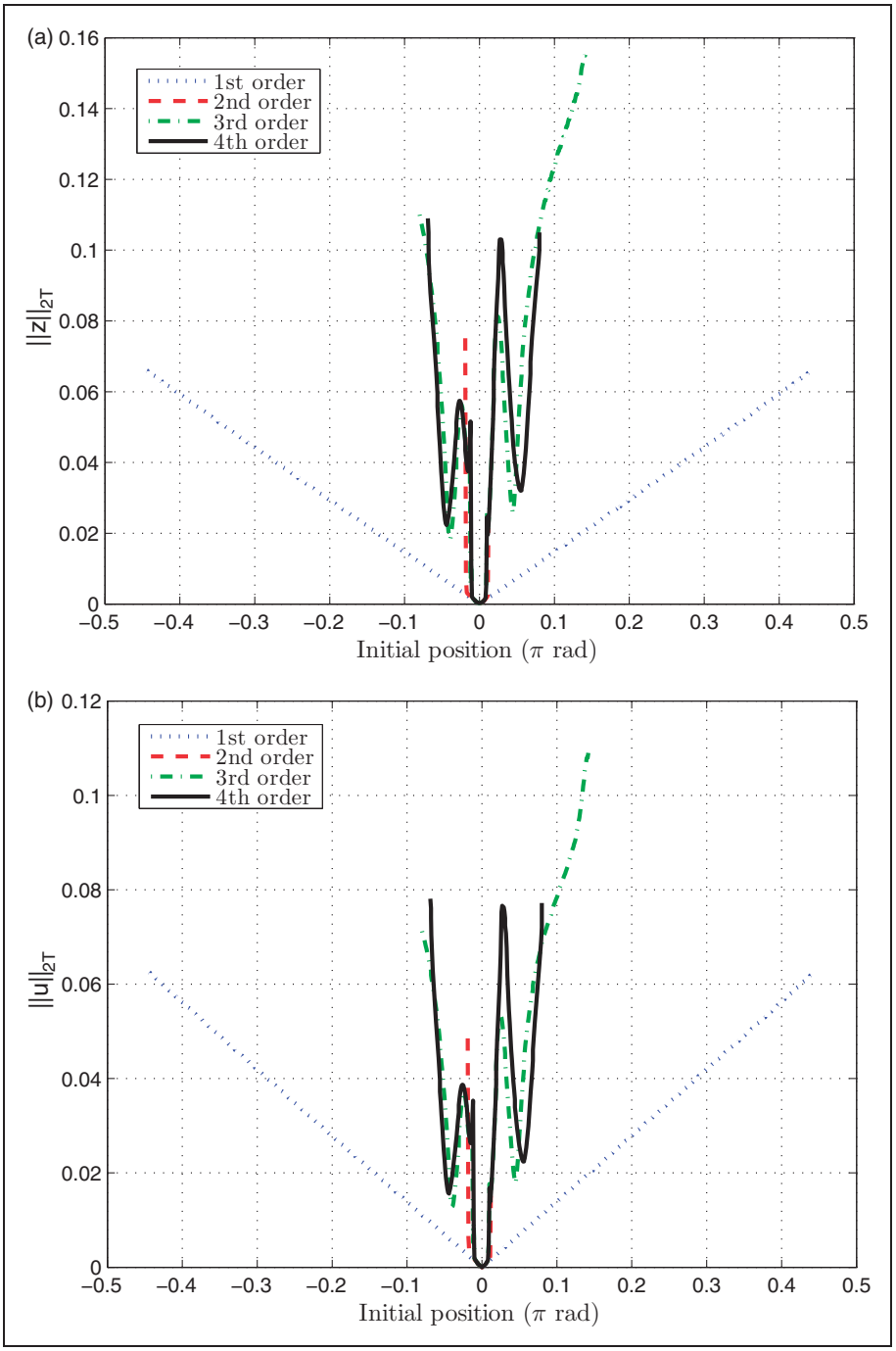

Figure 4. Relative performance for various initial values of σ for the output feedback controllers tracking an orbitally fixed direction. (a) $||\mathbf{z}||_{2T}$ response and (b) $||\mathbf{u}||_{2T}$ response.

practice (e.g. detumbling). There are also several resonances apparent in the results. The nonlinear output feedback controllers have extremely small domains of attraction, as depicted in Figure 6.

Comments on instability of higher-order solutions. The higher-order solutions to the output feedback problem seem to have some significant stability issues. It is speculated that part of this is due to the inverted matrix present in the observer gain. For the linear output feedback case, there is no worry that the inverse matrix approaches a singularity for any state in the state space. However, for the higher-order controllers, there is a problem: the matrix to be inverted (see equation (46)) is dependent on the states. In this case, it is certainly within the realm of possibility that the matrices that make up the term to be inverted will be singular at one or more points in the state space. Given the discrete nature of the integration scheme, even a close pass near any of these singularities can be enough to destabilize the system in an unrecoverable way. In future analyses, it may be beneficial to attempt to find the Taylor series expansion of this inverted term *after* the inversion.

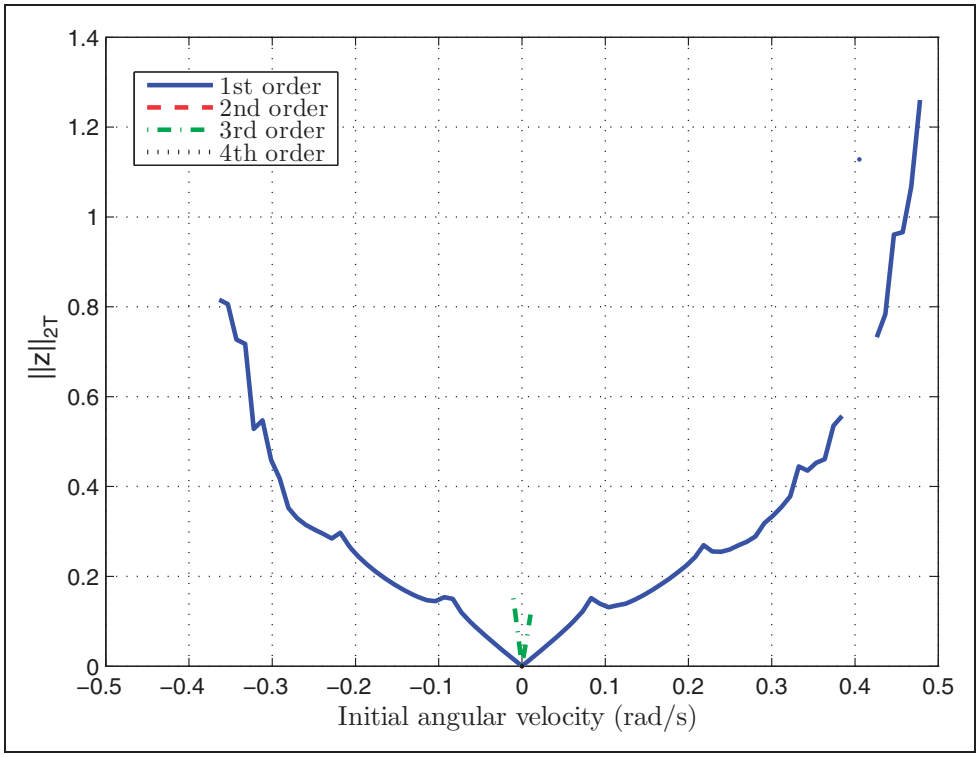

Figure 5. $||\mathbf{z}||_{2T}$ response for various initial values of σ for the output feedback controllers tracking an orbitally fixed direction.

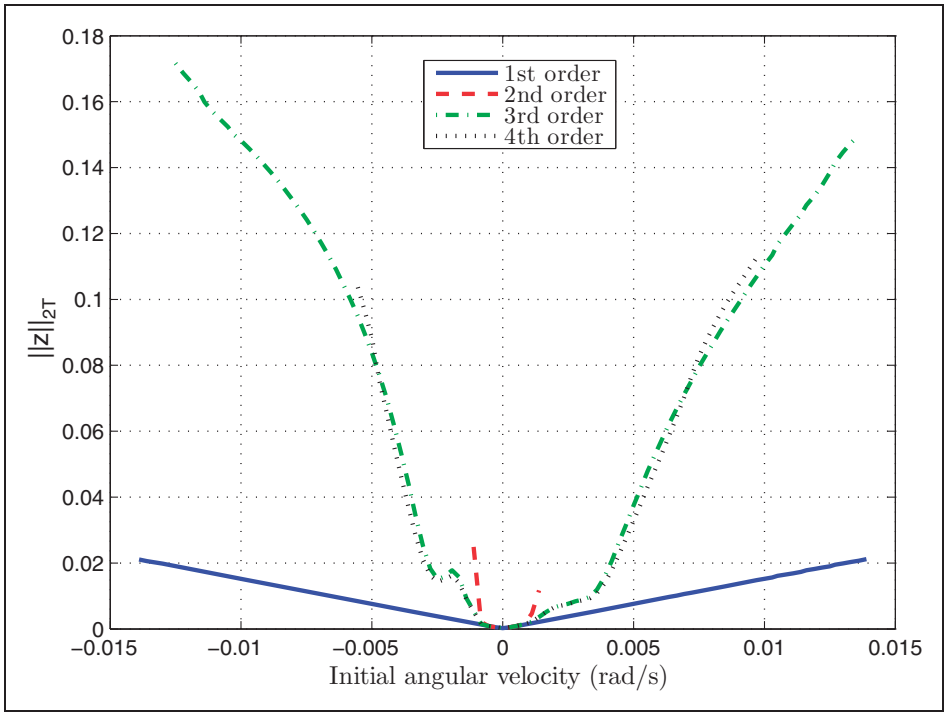

Figure 6. $||\mathbf{z}||_{2T}$ response for various initial values of ω_e for the output feedback controllers tracking an orbitally fixed direction – detail.

It should also be noted that in order for the quantities V and U to furnish solutions to the control problem, they must satisfy $V(\mathbf{x}) > 0$, $U(\mathbf{x}) > 0$, and $U(\mathbf{x}) - V(\mathbf{x}) > 0 \quad (\mathbf{x} \neq \mathbf{0})$. For the linear controllers, these three quantities are quadratic forms and it is relatively easy to satisfy the three positivity conditions. For the higher-order solutions, satisfaction of the positivity conditions becomes difficult

Table 1. Orbital frame tracking controller response to magnetic torque.

	Order	$\|\|\omega_e\|\|_{2T}$	$\|\|\phi\|\|_{2T}$	$\|\|\mathbf{u}\|\|_{2T}$	$\|\|\mathbf{w}_1\|\|_{2T}$	$\|\|\mathbf{z}\|\|_{2T}$	CL-gain
State ($\gamma = 2$)	1	1.83×10^{-4}	1.45×10^{-1}	4.23×10^{-4}	4.21×10^{-4}	5.57×10^{-4}	1.32
	2	1.83×10^{-4}	1.45×10^{-1}	4.23×10^{-4}	4.21×10^{-4}	5.57×10^{-4}	1.32
	3	1.83×10^{-4}	1.45×10^{-1}	4.23×10^{-4}	4.21×10^{-4}	5.57×10^{-4}	1.32
	4	1.83×10^{-4}	1.45×10^{-1}	4.23×10^{-4}	4.21×10^{-4}	5.57×10^{-4}	1.32
Output ($\gamma = 20$)	1	2.28×10^{-4}	1.78×10^{-1}	4.24×10^{-4}	4.21×10^{-4}	6.15×10^{-3}	1.46
	2	2.28×10^{-4}	1.78×10^{-1}	4.24×10^{-4}	4.21×10^{-4}	6.15×10^{-3}	1.46
	3	2.28×10^{-4}	1.78×10^{-1}	4.24×10^{-4}	4.21×10^{-4}	6.15×10^{-3}	1.46
	4	2.28×10^{-4}	1.78×10^{-1}	4.24×10^{-4}	4.21×10^{-4}	6.15×10^{-3}	1.46

except in small regions of the state space about the origin.

Input–output response

Having considered the response to initial conditions, the input–output response is now treated. In this case, it will be possible to verify the performance of the controllers against the nonlinear $\mathcal{H}_\infty$ gain parameter γ that was used to create them. The base orbital simulation parameters are as follows: the spacecraft is in a circular orbit at an altitude of 450 km with an inclination of $i = 87^\circ$. The right ascension of the ascending node and the initial argument of latitude are both taken to be zero. The spacecraft generates a magnetic dipole of $\mathbf{m} = [0.1\ 0.1\ 0.1]^T$ Am^2, expressed in the body-fixed frame. Table 1 summarizes the results of the simulation.

The relative changes in response to magnetic disturbances are negligible. No improvement is seen for any of the higher-order controllers in either the state feedback or output feedback case. Figure 7 demonstrates the first-order output feedback system response over one orbit.

Conclusion

The purpose of this paper has been to explore the application of nonlinear $\mathcal{H}_\infty$ control to the attitude control problem for Earth-pointing spacecraft. Specifically, an extension of the linear $\mathcal{H}_\infty$ control design technique has been used which involves replacing the AREs central to $\mathcal{H}_\infty$ control with general nonlinear Hamilton–Jacobi inequalities.

This paper began by presenting the development of the kinematics and dynamics governing the motion of an Earth-pointing spacecraft in a circular orbit. The kinematics were described using the MRPs, and the dynamics were described relative to the orbital frame. Next, the form of controllers was determined that can stabilize a given nonlinear plant, subject to a norm constraint on the input–output map, in both the state feedback and the output feedback cases. The form of the state estimator in the output feedback case was also provided. From this, a linearized (first-order) controller was provided. Then, higher-order controllers (up to order four) were found through an iterative process of solving the terms in the two HJEs that arose from a Taylor series representation of the system dynamics and Hamiltonian functions. These controllers were evaluated on both an input–output basis and an initial condition basis.

It was found that the linearized feedback controllers performed as well as or better than the higher-order nonlinear controllers in both the state feedback and the output feedback cases, when subjected to varying initial conditions. These linearized controllers proved to have regions of stability that were at least as great as those for the nonlinear controllers. The nonlinear controllers performed especially poorly in the output feedback case. It is thought that this may be due to the matrix inverse present in the estimator gain expression. The matrix to be inverted is dependent on the estimated state for controllers of order two or higher, meaning that one cannot guarantee that it remains nonsingular for all possible estimated states. Indeed, this proved to be a significant problem in the initial condition simulations. When comparing the input–output response of the controllers subject to magnetic torques, it was found that controllers of every order performed nearly identically, bolstering the claim that the linearized result is close to optimal.

This paper demonstrates that linear feedback, which is often selected as the control mechanism of choice due to its simplicity and the extensive background theory available, appears to be nearly optimal for the Earth-pointing attitude control problem subject to the $\mathcal{H}_\infty$ design constraint. This somewhat surprising result clearly shows the importance of testing proposed control schemes before selecting a control that may be unnecessarily complex.

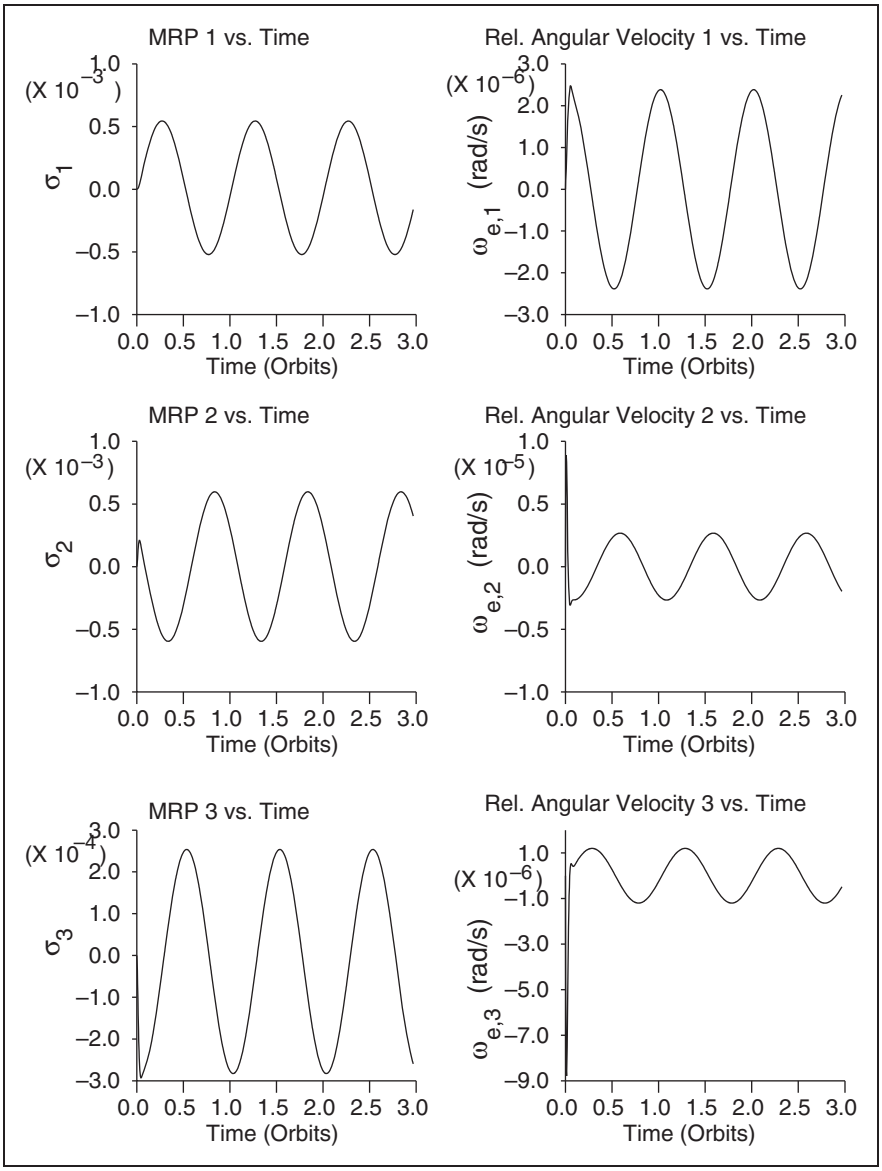

Figure 7. First-order output feedback orbital frame tracking controller response to magnetic torque.

Funding

This research was funded by the Dean's Strategic Fund, Faculty of Applied Science and Engineering, University of Toronto.

Conflict of interest

None declared.

References

1. Karlgaard CD and Schaub H. Nonsingular attitude filtering using modified Rodrigues parameters. *J Astronaut Sci* 2009; 57: 777–791.
2. Tsiotras P. Stabilization and optimality results for the attitude control problem. *J Guid Control Dyn* 1996; 19: 772–779.
3. Zames G. Feedback and optimal sensitivity: model reference transformations, multiplicative seminorms, and approximate inverses. *IEEE Trans Automat Control* 1981; 26: 301–320.
4. Doyle JC, Glover K, Khargonekar PP, et al. State-space solutions to standard $\mathcal{H}_2$ and $\mathcal{H}_\infty$ control problems. *IEEE Trans Automat Control* 1989; 34: 831–847.
5. van der Schafts AJ. L_2-gain analysis of nonlinear systems and nonlinear state-feedback $\mathcal{H}_\infty$ control. *IEEE Trans Automat Control* 1992; 37: 770–784.
6. Pavel L and Fairman FW. Nonlinear $\mathcal{H}_\infty$ control: a *J*-dissipative approach. *IEEE Trans Automat Control* 1997; 42: 1636–1653.
7. Al'brekht EG. On the optimal stabilization of nonlinear systems. *J Appl Math Mech* 1961; 25: 1254–1266.
8. Lukes DL. Optimal regulation of nonlinear dynamical systems. *SIAM J Control* 1969; 7: 75–100.
9. Garrard WL. Suboptimal feedback control for nonlinear systems. *Automatica* 1972; 8: 219–221.
10. Garrard WL and Jordan JM. Design of nonlinear automatic flight control systems. *Automatica* 1977; 13: 497–505.

11. LeBel S and Damaren CJ. Analytical solutions to approximations of the Hamilton-Jacobi equation applied to satellite attitude control. In: *Proceedings of the AIAA guidance, navigation, and control conference,* Toronto, ON, Canada, 2–5 August 2010.
12. Hughes PC. *Spacecraft attitude dynamics*. Mineola, New York, USA: Dover Publications, 2004.
13. Tanygin S. Attitude parameterizations as higher-dimensional map projections. *J Guid Control Dyn* 2012; 35: 13–24.
14. Tsujii S, Bando M and Yamakawa H. Spacecraft formation flying dynamics and control using the geomagnetic Lorentz force. *J Guid Control Dyn* 2013; 36: 136–148.
15. Lu W-M and Doyle JC. $\mathcal{H}_\infty$ control of nonlinear systems via output feedback: a class of controllers. In: *Proceedings of the 32nd IEEE conference on decision and control,* San Antonio, TX, USA, December 1993, pp.166–171. USA: IEEE.